

Analysis of a Spatially Correlated Vehicular Network Assisted by Cox-distributed Vehicle Relays

Chang-Sik Choi and François Baccelli

Abstract—In vehicle-to-all (V2X) communications, roadside units (RSUs) play an essential role in connecting various network devices. In some cases, users may not be well-served by RSUs due to congestion, attenuation, or interference. In these cases, vehicular relays associated with RSUs can be used to serve those users. This paper uses stochastic geometry to model and analyze a spatially correlated heterogeneous vehicular network where both RSUs and vehicular relays serve network users such as pedestrians or other vehicles. We present an analytical model where the spatial correlation between roads, RSUs, relays, and users is systematically modeled via Cox point processes. Assuming users are associated with either RSUs or relays, we derive the association probability and the coverage probability of the typical user. Then, we derive the user throughput by considering interactions of links unique to the proposed network. This paper gives practical insights into designing spatially correlated vehicular networks assisted by vehicle relays. For instance, we express the network performance such as the user association, SIR coverage probability, and the network throughput as the functions of network key geometric variables. In practice, this helps one to optimize the network so as to achieve ultra reliability or maximum user throughput of a spatially correlated vehicular networks by varying key aspects such as the relay density or the bandwidth for relays.

Index Terms—Spatially correlated vehicular networks, Vehicle relays, Performance analysis, Stochastic geometry, Cox point process

I. INTRODUCTION

A. Background and Motivation

Recent innovations have made it possible for vehicles to play new roles in urban environments, extending their traditional transportation role [2]–[4]. Vehicles will participate in various road safety and efficiency applications by communicating with neighboring vehicles, pedestrians, traffic lights, and Internet-of-Things (IoT) devices [2], [4]. Advanced vehicles and their sensors provide ways to improve not only their own safety, but also that of others such as pedestrians [5], [6]. This innovative use of vehicles requires reliable communications among network entities such as vehicles, base stations, smart sensors, and pedestrians [6]–[8].

Vehicular networks featuring reliable and high capacity links can be achieved by base stations close to roads, namely RSUs. Connected to the core network through backhaul, RSUs will host advanced V2X applications [5], [9]. As the number of network users increases and vehicular networks have more services, some network users relying only on RSUs may

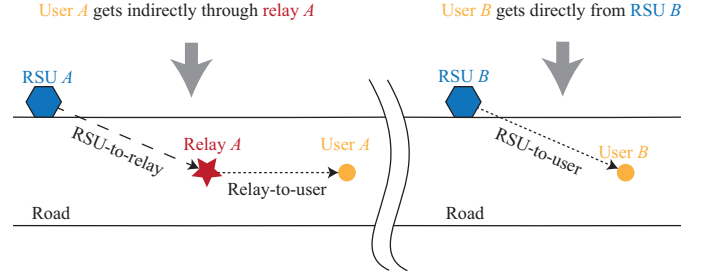


Fig. 1. Illustration of the proposed vehicular network with RSUs, relays, and users. Users may get messages directly from RSUs (right) or via relays (left).

experience limited coverage because of data congestion, load unbalancing, signal attenuation, and high interference.

To fight against these limitations, various technologies have been developed and among that, this paper focuses on the use of vehicular relays [10], [11]. Specifically, RSU-operated vehicular relays will reshape the topology of vehicular networks to increase the reliability and throughput of network [10], [11]. For instance, users in dense areas can communicate each other via relays, avoiding extra delays occurring at RSUs; or relays can forward important messages to the users far away from RSUs. Fig. 1 illustrates such an example.

Focusing on the network topology and the geometric interaction between network elements, this paper studies the fundamental performance of a spatially correlated two-tiered heterogeneous vehicular network with RSUs and relays operated through them. (Fig. 1.) In particular, to describe the spatial interaction between RSUs, relays, and users all at the same time, we employ a stochastic geometry framework [12]–[15]. In particular, many studies used analytic models based on the Poisson point processes [16]–[19] where network elements can be well captured as spatially independent components. Recently, Cox point processes has been employed to describe the locations of spatially correlated network elements such as roads, vehicles, and pedestrians. Specifically, the Cox models were extensively used in various papers including [20]–[34] to analyze the basic network performance with vehicle transmitters and vehicle receivers.

Continuing this line of work, this paper also employs Cox point processes to describe the locations of RSUs, users, and vehicle relays, all within the same road infrastructure. It is worth noting that, due to this practical representation of spatially correlated network elements—RSUs, vehicular relays, and users, the network performance improved by vehicle relays can be fairly and accurately analyzed. To the best of the authors’ knowledge, no prior work has addressed a system-

Chang-Sik Choi is with Hongik University, South Korea. François Baccelli is with Inria Paris and with Telecom Paris, France.(email: chang-sik.choi@hongik.ac.kr, francois.baccelli@inria.fr). This paper is an extension of our early work [1].

level analysis of a vehicular network with vehicle relays, especially by emphasizing the network topology produced by RSUs, vehicle relays, and network vehicle users, all of which must be located on the common road infrastructure.

B. Theoretical Contributions

1) *Modeling of a spatially correlated two-tier heterogeneous vehicular network:* In vehicular networks, network elements e.g., RSUs, vehicles transceivers, and pedestrians are all close to roads. In this paper, we focus on this geometric characteristic by modeling a road layout first as a Poisson line process and then distributing RSUs, vehicular relays, and users as Poisson point processes conditional on the line process. By constructing all elements conditionally on roads, we account for the fact that RSUs, relays, and users are located on roads and nowhere else. The proposed network modeling technique allows one to identify the geometric interaction of a two-tier heterogeneous vehicular network, especially between various communication links such as RSU-to-relay links, relay-to-user links, and RSU-to-user links. In contrast to our previous work [22], [23] where only a single set of vehicle transmitters is considered as a Cox point process, this work considers two sets of transmitters modeled as Cox point processes conditionally on a single road layout.

2) *Association behavior of users and coverage probability:* Motivated by basic safety messages transmitted from network elements and received by nearby users [35], [36], we assume that network users are associated with their closest RSUs or closest relays. We derive the association probability as a function of relay density and RSU density. The obtained probability describes the fraction of users associated with RSUs or with relays, at any given time. We show that the association probability is not given by a simple linear function because of the spatial correlation between RSUs and RSU-operated relays. Assuming frequency resources are separated for operating relays and for serving network users, we evaluate the coverage probability of the typical user as an integral function. See II for detail.

3) *Comprehensive analysis and design insights:* Taking into account the fact that relays are operated by RSUs and users are served by both relays and RSUs, we evaluate the effective throughput of the typical user in the proposed network. In particular, we get the user throughput formula leveraging (i) the throughputs of RSU-to-user links and relay-to-user links, respectively, (ii) the SIR distribution and throughput of RSU-to-relay links, (iii) the average number of network elements involved in the above links. Without ignoring the bottleneck resulting from the RSU-to-relay links, the throughput formula accurately describes the redistribution of the network payload achieved by spatially correlated relays in heterogeneous vehicular network architectures. In particular, we express the user throughput as a function of network parameters including frequency resources and densities of RSUs, relays, and users. As a result, it can be effectively used to design and build heterogeneous vehicular networks where spatially correlated network elements exist. For instance, leveraging the throughput expression, network operators can allocate

frequency resources to various links to optimize the network performance for given densities of RSUs, relays, and network users.

II. SYSTEM MODEL

This section gives the spatial model for RSUs, relays, and users. We then discuss the propagation model, the user association principle, and performance metrics.

A. Spatial Model for RSUs and Users

To represent road geometries in urban areas, we assume that the road layout is modeled as an isotropic Poisson line process Φ [14]. In the context of stochastic geometry such a model has been widely accepted for its analytical tractability [21], [22], [24]–[29]. Specifically, the Poisson line process is generated from a homogeneous Poisson point process on a cylinder set \mathcal{C} . Consider a Poisson point process Ξ of intensity λ_l/π on \mathcal{C} . Here λ_l (per km) is the mean number of road segments in a circle of radius 1 km.

Each of its point (r, θ) is mapped into a line on the Euclidean plane, where r corresponds to the distance from the origin to the line and θ corresponds to the angle between the line and the x -axis, measured in the counterclockwise direction [14].

Conditionally on each line $l(r, \theta) \in \Phi$, the locations of RSUs and network users, are modeled as independent one-dimensional Poisson point processes $S_{r, \theta}$ and $U_{r, \theta}$ of intensities μ_s and μ_u , respectively, where $\mu_u \gg \mu_s$. Here, μ_s is the mean number of RSUs on a road segment of 1 km and μ_r is the mean number of relays on a road segment of 1 km.

Collectively, the RSU point process S and the user point process U form Cox point processes constructed under an identical Poisson line process [23]. We have

$$S = \bigcup_{r_i, \theta_i \in \Phi} S_{r_i, \theta_i}, \quad (1)$$

$$U = \bigcup_{r_i, \theta_i \in \Phi} U_{r_i, \theta_i}. \quad (2)$$

Figs. 2 – 4 show the proposed network model having RSUs, vehicle relays, and network users, all located on the same road infrastructure. In Fig. 2, the road density is 2/km and it means there are 4 roads in a disk of radius 1 km on average. In Fig. 4, we use $\lambda_l = 10$, a very dense urban area with many roads. It is worth noting that RSUs, relays, and network users are all constrained by the common road infrastructure.

Remark 1. *It is important to mention that we take the the simplest approach to characterize spatially correlated component in a two-tier heterogeneous vehicular network. For instance, Ξ is a homogeneous Poisson point process of a constant intensity. Thus, we have an isotropic Poisson line process Φ on the Euclidean plane. Nevertheless, one can change it by considering dirac-delta measure across the angle of roads to create a Manhattan-like road layout. See [22]. A more realistic model obtained by changing the intensity measure of Ξ is left for future work.*

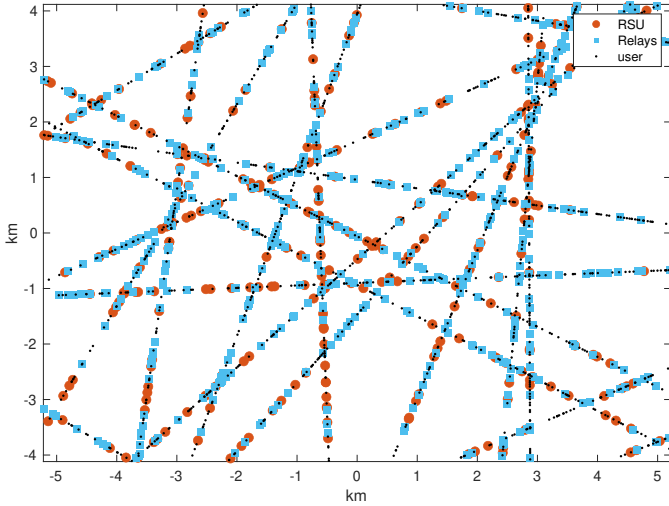


Fig. 2. Illustration of the proposed network where $\lambda_l = 2/\text{km}$, $\mu_s = 2/\text{km}$, $\mu_r = 4/\text{km}$, and $\mu_u = 10/\text{km}$.

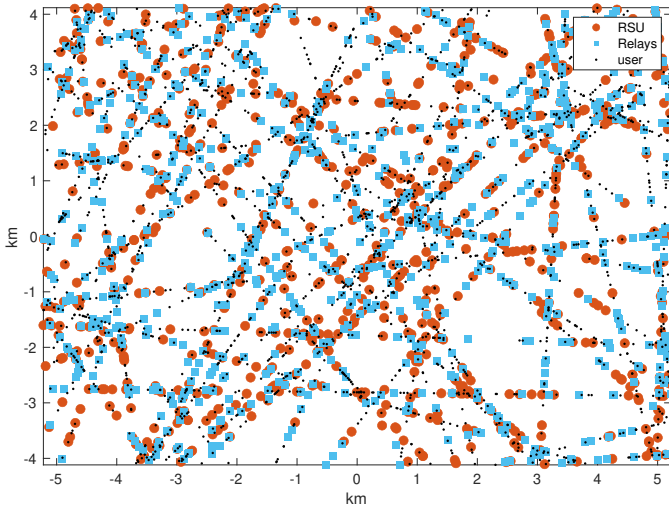


Fig. 3. Illustration of the proposed network where $\lambda_l = 5/\text{km}$, $\mu_s = 2/\text{km}$, $\mu_r = 2/\text{km}$, and $\mu_u = 5/\text{km}$.

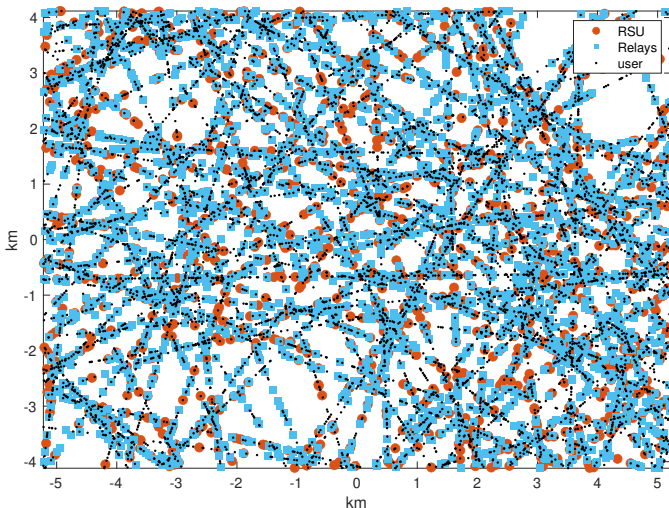


Fig. 4. Illustration of the proposed network where $\lambda_l = 10/\text{km}$, $\mu_s = 2/\text{km}$, $\mu_r = 4/\text{km}$, and $\mu_u = 10/\text{km}$.

B. Spatial Model for Relay and Reserved Spectrum

We assume that vehicular relays are wirelessly connected to RSUs and they serve network users [10], [36] as in Fig. 1. In the sequel, RSU-operated vehicular relays will be referred to relays.

Since relays are on roads too, we model the locations of relays as a Cox point process, denoted by R . Specifically, conditional on each road $l(r, \theta)$ created by the above Poisson line process Φ , the locations of relays on each road follow a Poisson point process $R_{r, \theta}$ of intensity μ_r . Following the notation of Eqs. (1) and (2), we let

$$R = \bigcup_{r_i, \theta_i \in \Phi} R_{r_i, \theta_i}. \quad (3)$$

It is important to note that the RSU point process S , the relay point process R , and the user point process U are all on the same line process Φ . As a result, our approach captures the fact that RSUs, relays, and users are all on the very same road structure. Fig. 2 shows the spatial distributions of the RSUs, relays, and network users in the proposed network.

To operate relays, network operators can employ various approaches. To maintain the tractability of our work, we consider the simplest assumption that the frequency resources for *operating* relays and the frequency resources for *serving* network users are separate. (See Fig. 1 where links are shown.) This is partly motivated by the radio resource management technique in practice [10], [36], where the frequency resources can be autonomously taken by vehicles or scheduled by RSUs. Specifically, to communicate with relays, RSUs use the spectrum f_2 of bandwidth W_2 . On the other hand, to serve network users on roads, RSUs and relays use the spectrum f_1 of bandwidth W_1 . In other words, we have three different types of communication links (i) RSU-to-user links, (ii) relay-to-user links, and (iii) RSU-to-relay links. Types (i) and (ii) use W_1 and Type (iii) uses W_2 .

Note that we assume that f_1 and f_2 do not overlap and that $W_1 + W_2 = W$ where W is the total available bandwidth. Table I shows the communication links and their corresponding resources.

Remark 2. In practical cases, users may experience limited coverage because of interference or attenuation. In the proposed architecture, RSUs configure relays to forward their messages to network users. To ensure reliable reception of messages at their final destinations, we assume that the initial links of such relaying, namely RSU-to-relay communications occupy a reserved spectrum f_2 of bandwidth W_2 . For the rest of the communication links in the proposed two-tier heterogeneous vehicular networks, e.g., relay-to-user and RSU-to-user links, we consider those links use a spectrum f_1 of bandwidth W_1 . Therefore, there is no co-channel interference between RSU-to-relay communications and the rest of the communications in the proposed architecture. Motivated by current standard implementation [10], [36], [37], we assume that RSU-to-user and relay-to-user links exist on the same spectrum and thus there is co-channel interference between them.

TABLE I
SPECTRUM USAGE

Communication link types	Bandwidth
RSU-to-user links	W_1
relay-to-user links	W_1
RSU-to-relay links	W_2

C. Relay and User Mobility

In vehicular networks, RSUs do not move while relays and network users move along the roads. We assume that relays and users move along the line they are located on and that they choose their speeds uniformly out of a given distribution. Specifically, each relay independently selects its own speed on the interval $[v_{r,\min}, v_{r,\max}]$ uniformly at random. Each network user selects its own speed on the interval $[v_{u,\min}, v_{u,\max}]$ uniformly at random.

Example 1. *One can relax the above mobility assumption. An example is that where relays and users on each road choose their own speeds out of standard normal distributions. Based on the displacement theorem [38], the Poisson property of the relay and user point processes is preserved over time. Thus, the relay and user point process are still given by time invariant Cox point processes. This shows that the proposed mobility model and the corresponding analysis in this paper generalize to various mobility cases.*

D. Relay Association and User Association

With regards to relays, we assume that relays are associated with their closest RSUs. The RSU-to-relay communication links are established between RSUs and relays; and then, these relays forward messages from RSUs to nearby users. See Fig. 1. Combined with the separate spectrum usage given in II-B, the nearest association is a basis for the reliable reception of forwarded messages at the final destinations.

With regards to users, we assume that each user is associated with its closest transmitter, namely either an RSU or a relay. This is based on practical use cases [5], [7], [8], [35] where network users are configured to connect with their nearest transmitters. The bottom figures of Fig. 2 shows the user association map as the Voronoi tessellation, illustrated by solid blue lines. The centers of the Voronoi cells are the transmitter point process, i.e., $S + R$. The cells are the user association map. Users are connected to transmitters at their cell centers.

As the number of transmitters increase, the average size of cells decreases and thus the average number of users associated with each transmitters.

Remark 3. *[1] studied various user association techniques including the maximum average receive signal power association and the nearest user association. In this paper, motivated by the various distance-critical safety V2X applications, we focus on the nearest user association principle. Nevertheless, the formulas and analysis given in this paper can be readily used to analyze the maximum average receive signal power association simply by changing the coefficients of transmit powers, exploiting techniques in [18], [39], [40].*

E. Propagation Model

Consider a receiver located at a distance d from its transmitter. In the proposed heterogeneous vehicular network, transmitters are either RSUs or relays. We assume rich scattering around the network users [41] and a power-law path loss function [35]. The received signal power at the receiver is assumed to be of the form $pHL(d)$ where $p = \{p_s, p_r\}$ is the received signal powers at 1 meter from an RSU or a relay, respectively. H represents Rayleigh fading, modeled by an independent exponential random variable with average one, and $L(d)$ is the path loss over distance $d \geq 1$. We assume that the transmit powers for RSUs and relays are given by p_s and p_r , respectively.

For path loss, we address that the path loss shows different characteristics, depending on the relative locations of transmitters and receivers, or more precisely, on whether transceivers are on the same road or not [42]. For tractability, we use a simple path loss model where the path loss $L(d)$ over a distance d is

$$L(d) = \begin{cases} d^{-\alpha} & \text{on the same road,} \\ d^{-\beta} & \text{on different road,} \end{cases} \quad (4)$$

where $2 < \alpha \leq \beta$.

F. Performance Metrics

This paper analyzes the performance seen by the network users. We first derive the coverage probability of the typical user and then derive the coverage probability of the typical relay. Then, using both, we derive the user effective throughput.

1) *User Coverage Probability:* To analyze the coverage probability of the typical user, we use the Palm distribution of the user point process, $\mathbf{P}_U^0(\cdot)$. This features a typical user at the origin. Therefore a line $l(0, \theta_0)$ almost surely exists with a RSU point process S_{0, θ_0} , and a relay point process R_{0, θ_0} on it [20], [23]. The coverage probability of the typical user $\mathbf{P}_U^0(\text{SIR} > \tau)$ is given by

$$\mathbf{P}_U^0 \left(\frac{pHL(\|X^*\|)}{\sum_{X_j \in S+R \setminus B(\|X^*\|)} pX_j H_j L(\|X_j\|)} > \tau \right), \quad (5)$$

where p is the transmit power of the association transmitter which could be either p_s or p_r depending on the user association. We denote by $B_0(\|X^*\|)$ the ball of radius $\|X^*\|$ centered at the origin; we also write $B_0(r) \equiv B(r)$. Here, τ is the SIR threshold. Based on the association principle of above, the association transmitter X^* is given by

$$X^* = \arg \min_{X_k \in S_{0, \theta_0} + R_{0, \theta_0} + S + R} \|X_k\|. \quad (6)$$

Here, the association transmitter is selected out of the point processes: S_{0, θ_0} , R_{0, θ_0} , S , and R . When the association transmitter is a RSU, we write $X^* = X_S^*$. When the association transmitter is a relay, we write $X^* = X_R^*$.

Based on the association, users can be divided into two types, namely those associated with RSUs and those with relays. We need to separately evaluate each type as follows:

$$\mathbf{P}_U^0(\text{SIR}_{S \rightarrow U} > \tau) := \mathbf{P}_U^0(\text{SIR} > \tau | X^* = X_S^*), \quad (7)$$

$$\mathbf{P}_U^0(\text{SIR}_{R \rightarrow U} > \tau) := \mathbf{P}_U^0(\text{SIR} > \tau | X^* = X_R^*), \quad (8)$$

where the former denotes the coverage probability of the typical relay-associated user and the latter denotes that of the typical RSU-associated user.

2) *Relay Coverage Probability*: To analyze the SIR of the typical relay, we consider the Palm distribution of the relay point process. The coverage probability of the typical relay, $\mathbf{P}_R^0(\text{SIR}_{S \rightarrow R} > \tau)$ is given by

$$\mathbf{P}_R^0 \left(\frac{p_s H L(\|X_S^*\|)}{\sum_{X_j \in S \setminus B(\|X_S^*\|)} p_s H_j L(\|X_j\|)} > \tau \right), \quad (9)$$

where X_S^* is the RSU closest to the typical relay located at the origin under the Palm distribution of the relay point process R . Since RSU-to-relay communications are assumed to occur over a frequency bandwidth of W_2 , it is worth noting that the RSU-to-relay links do not interfere with RSU-to-user and relay-to-user links.

3) *Throughput*: Using the coverage probabilities above, we derive the throughput of the typical user. In the proposed vehicular network where relays are operated by RSUs over a separate wireless resource W_2 , the throughput is not just a simple function of the SIR distribution of the typical user. The precise definition of the user throughput will be given in Section V.

III. ASSOCIATION PROBABILITY

Each user has either a RSU association or a relay association, depending on its distances to RSUs and relays. Here, we study the probability that the typical user is associated with either an RSU or a relay. The association probability is derived under the Palm distribution of the user point process. The association probability also corresponds to the fraction of network users associated with RSUs and with relays, respectively.

Lemma 1. *The probability that the typical user is associated with an RSU is given by Eq. (10) Likewise, the probability that the typical user is associated with a relay is $\mathbf{P}(A_r) = 1 - \mathbf{P}(A_s)$.*

Proof: See [1, Theorem 1]. ■

Fig. 5 shows that the derived association probability derived in Lemma 1 matches the association probability numerically obtained by the Monte Carlo simulations. We use $\lambda_l = 2/km$. We see that as the density of relays increases, the relay association probability increases. Since the user association is based on distance, it is possible that users are associated with RSUs or relays on different lines. We will use the derived association probability to evaluate the coverage probability of the typical user. In addition, we show that the association probability is not given by a simple ratio of densities. This contrasts to the association probability of users in the heterogeneous networks modeled by Poisson point processes [18]. This occurs because of the spatial correlation between RSUs and relays.

Theorem 1. *The mean number of users associated to the typical RSU is $\frac{\mu_u}{\mu_s} \mathbf{P}_u(A_s)$ and the mean number of users associated to the typical relay is $\frac{\mu_u}{\mu_r} \mathbf{P}_u(A_r)$. The mean number of relays associated to the typical RSU is $\frac{\mu_r}{\mu_s}$.*

Proof: Consider a factor graph with an edge from each user to its association RSU or relay. From the mass transport principle [38],

$$\lambda_l \mu_u \mathbf{P}_U^0(A_s, E) = \lambda_l \mu_s d_{in}, \quad (11)$$

where the left-hand side is the mean mass sent by the users to their association RSUs on the same lines, whereas the right-hand side is the mean mass received by the RSUs from their associated users on the same lines. $\lambda_l \mu_s$ is the spatial density of RSUs and d_{in} is the mean number of same-line users associated to the typical RSU under the Palm distribution of S . Similarly, considering users and their associated RSUs on different lines, we have

$$\lambda_l \mu_u \mathbf{P}_U^0(A_s, E^c) = \lambda_l \mu_s d'_{in}, \quad (12)$$

where the left-hand side is the mean mass out of the users and the right-hand side is the mean mass received by the RSUs: d'_{in} is the mean number of different-line users associated to the typical RSU. As a result, the mean number of users per RSU is $d'_{in} + d_{in} = \mu_u \mathbf{P}_U^0(A_s) / \mu_s$. Similarly, the mean number of users per relay is $\mu_u \mathbf{P}_U^0(A_r) / \mu_r$. Finally, the mean number of relays per RSU is μ_r / μ_s . ■

The above proposition is essential to address the impact of RSU-to-relay links to the system performance. We use the above expression in the derivation of the user throughput in Section V.

IV. COVERAGE PROBABILITY OF USER AND RELAY

In Section IV-A, we first evaluate the coverage probability of the typical user under the Palm distribution of the user point process, by leveraging the facts that the network users are connected with their closest RSUs or relays and that RSU-to-user links interfere with relay-to-user links and vice versa. Then, in Section IV-B we independently derive the coverage probability of the typical relay under the Palm distribution of the relay point process. The coverage probabilities of Sections IV-A and IV-B impacts the throughput of the network that we will see in Section V.

A. Coverage Probability of the Typical User

This section gives the coverage probability of the typical user. Note all RSUs and relays are assumed to have users to serve with high probability. We denote by γ the ratio of relay transmit power to the RSU transmit power, $\gamma = p_r / p_s$. As in Section III, let E be the event that the association transmitter and the typical user are on the same line. We denote by A_s the event that the association transmitter is an RSU and by A_r the event that the association transmitter is a relay.

Theorem 2. *The coverage probability of the typical user is $\mathbf{P}_U^0(\text{SIR} > \tau, E, A_s) + \mathbf{P}_U^0(\text{SIR} > \tau, E, A_r) + \mathbf{P}_U^0(\text{SIR} > \tau, E^c, A_s) + \mathbf{P}_U^0(\text{SIR} > \tau, E^c, A_r)$, given by Eq. (13) – (16), respectively where*

$$G_1(r, a, b) = 2\mu_s e^{-2r\mu_s - 2\mu_s \int_r^\infty \frac{\tau r^\alpha u^{-\alpha}}{a + \tau r^\alpha u^{-\alpha}} du} e^{-2\mu_r \int_r^\infty \frac{\tau r^\alpha u^{-\alpha}}{b + \tau r^\alpha u^{-\alpha}} du},$$

$$\begin{aligned} \mathbf{P}(A_s) = & \int_0^\infty 2\mu_s \exp\left(-2(\mu_s + \mu_r)r - 2\lambda_l \int_0^r 1 - e^{-2(\mu_s + \mu_r)\sqrt{r^2 - u^2}} du\right) dr \\ & + 4\mu_s \lambda_l \int_0^\infty \int_0^{\pi/2} r e^{-2r(\mu_s + \mu_r) - 2r(\mu_s + \mu_r) \sin(\theta) - 2\lambda_l \int_0^r 1 - \exp(-2(\mu_s + \mu_r)\sqrt{r^2 - u^2}) du} d\theta dr. \end{aligned} \quad (10)$$

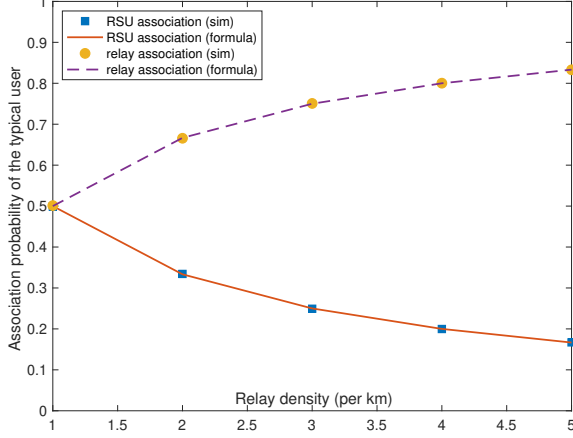


Fig. 5. Illustration of the association probability of the typical user. The derived formula of Lemma 1 matches the simulation results. We use $\lambda_l = 2/\text{km}$ and $\mu_s = 1/\text{km}$.

$$\begin{aligned} G_2(r, v, a, b) = & e^{-2(\mu_s + \mu_r)\sqrt{r^2 - v^2}} \\ & e^{-2\mu_s \int_0^\infty \frac{\tau r^\alpha (v^2 + u^2)^{-\beta/2}}{\sqrt{r^2 - v^2} (a + \tau r^\alpha (v^2 + u^2)^{-\beta/2})} du} \\ & e^{-2\mu_r \int_0^\infty \frac{\tau r^\alpha (v^2 + u^2)^{-\beta/2}}{\sqrt{r^2 - v^2} (b + \tau r^\alpha (v^2 + u^2)^{-\beta/2})} du}, \\ G_3(r, v, a, b) = & e^{-2\mu_s \int_0^\infty \frac{\tau r^\alpha (v^2 + u^2)^{-\beta/2}}{a + \tau r^\alpha (v^2 + u^2)^{-\beta/2}} du} \\ & e^{-2\mu_r \int_0^\infty \frac{\tau r^\alpha (v^2 + u^2)^{-\beta/2}}{b + \tau r^\alpha (v^2 + u^2)^{-\beta/2}} du}. \end{aligned}$$

On the other hand, we also have

$$\begin{aligned} H_1(r, a, b) = & e^{-2\mu_s r - 2\mu_s \int_r^\infty \frac{\tau r^\beta u^{-\alpha}}{a + \tau r^\beta u^{-\alpha}} du} \\ & e^{-2\mu_r \int_r^\infty \frac{\tau r^\beta u^{-\alpha}}{b + \tau r^\beta u^{-\alpha}} du}, \\ H_2(r, v, a, b) = & e^{-2(\mu_s + \mu_r)\sqrt{r^2 - v^2}} \\ & e^{-2\mu_s \int_0^\infty \frac{\tau r^\beta (v^2 + u^2)^{-\beta/2}}{\sqrt{r^2 - v^2} (a + \tau r^\beta (v^2 + u^2)^{-\beta/2})} du} \\ & e^{-2\mu_r \int_0^\infty \frac{\tau r^\beta (v^2 + u^2)^{-\beta/2}}{\sqrt{r^2 - v^2} (b + \tau r^\beta (v^2 + u^2)^{-\beta/2})} du}, \\ H_3(r, v, a, b) = & e^{-2\mu_s \int_0^\infty \frac{\tau r^\beta (v^2 + u^2)^{-\beta/2}}{a + \tau r^\beta (v^2 + u^2)^{-\beta/2}} du} \\ & e^{-2\mu_r \int_0^\infty \frac{\tau r^\beta (v^2 + u^2)^{-\beta/2}}{b + \tau r^\beta (v^2 + u^2)^{-\beta/2}} du}, \end{aligned}$$

$$\begin{aligned} H_4(r, c) = & \int_0^{\pi/2} 4\lambda_l c r e^{-2r(\mu_s + \mu_r) \sin(\theta)} \\ & e^{-2c \int_r^\infty \frac{\tau r^\beta (r^2 \cos^2(\theta) + v^2)^{-\beta/2}}{1 + \tau r^\beta (r^2 \cos^2(\theta) + v^2)^{-\beta/2}} dv} d\theta. \end{aligned}$$

In above, we derived the coverage probability of the typical user at the origin. Yet, the result is applicable to all the users in the network.

Remark 4. In Theorem 2, we analyze the SIR of the typical user located at the origin by using the Palm distribution of the user point process. Since the user point process is time invariant ergodic Poisson point process, the obtained formula corresponds to the spatial average of SIRs of all the users in the network [38], [43]. In other words, it corresponds to the statistic of the SIRs of all users in a large ball, at any given time. In addition, since the user point process is a time-invariant and ergodic Poisson point process, the coverage probability of the typical user coincides with the time average of the coverage probability of a specific user, obtained over a very long time [44].

Fig. 6 shows that the derived coverage probability of the typical user matches the numerical results obtained by Monte Carlo simulations, performed under various network parameters. In Figs. 7 – 9, we show only analytical results. Note that in the top figure of Fig. 7, the SIR curve slightly changes as the density of the relays varies. In the low SIR regime, the SIR curve slightly decreases as we increase the number of relays. This is because, in the low SIR regime, users are more likely to be associated with transmitters on lines that are different from the ones of users, and the received signal powers from the association transmitters are moderately dominated by the interference from the other transmitters. On the other hand, in the high SIR regime, the SIR curve increases as the number of relays increases. This is because, in the high SIR regime, users are more likely to be associated with the transmitters on the lines that are the same as the ones of users, and therefore the received signal powers dominate the interference. Nevertheless, it is worthwhile to mention that increasing the relay density does not always increase the SIR curve in some range of parameters. Especially when the relay or RSU density is very high, transmitters and receivers may be very close to each other and thus the power-law path loss function of this paper should be replaced with a truncated version, e.g., $L(d) = \min\{1, d^{-\alpha} \text{ or } d^{-\beta}\}$, to account for near field effect. The analysis with a truncated power-law path loss model is left for future work. In the right picture of Fig. 7, we increase the line density to show the change of the SIR curve. Although μ_s and μ_r are equal to one, the number of RSUs or relays $\lambda_l \mu_s / \pi$ or $\lambda_l \mu_r \pi$ respectively increases as λ_l increases. Therefore, the increment of the interference dominates the increment of the

$$\int_0^\infty G_1(r, a, b) e^{-2\lambda_l \int_0^r 1 - G_2(r, v, a, b) dv - 2\lambda_l \int_r^\infty 1 - G_3(r, v, a, b) dv} dr \Big|_{a=1, b=\frac{1}{\gamma}} \quad (13)$$

$$\int_0^\infty G_1(r, a, b) e^{-2\lambda_l \int_0^r 1 - G_2(r, v, a, b) dv - 2\lambda_l \int_r^\infty 1 - G_3(r, v, a, b) dv} dr \Big|_{a=\gamma, b=1} \quad (14)$$

$$\int_0^\infty H_1(r, a, b) e^{-2\lambda_l \int_0^r 1 - H_2(r, v, a, b) dv} e^{-2\lambda_l \int_r^\infty 1 - H_3(r, v, a, b) dv} H_4(r, c) dr \Big|_{a=1, b=\frac{1}{\gamma}, c=\mu_s} \quad (15)$$

$$\int_0^\infty H_1(r, a, b) e^{-2\lambda_l \int_0^r 1 - H_2(r, v, a, b) dv} e^{-2\lambda_l \int_r^\infty 1 - H_3(r, v, a, b) dv} H_4(r, c) dr \Big|_{a=\gamma, b=1, c=\mu_r} \quad (16)$$

$$\prod_{r_i, \theta_i} \left(\mathbf{E} \left[\prod_{T_j \in S_{0,0}} \frac{1}{1 + p_s s L(\|r_i \vec{e}_{i,1} + T_j \vec{e}_{i,2}\|)} \right] \mathbf{E} \left[\prod_{T_j \in R_{0,0}} \frac{1}{1 + p_r s L(\|r_i \vec{e}_{i,1} + T_j \vec{e}_{i,2}\|)} \right] \right) \quad (17)$$

$$4\lambda_l \mu_s r \int_0^{\pi/2} e^{-2r(\mu_s + \mu_r) \sin(\theta) - \int_r^\infty \sin(\theta) \frac{2\mu_s s p_s (r^2 \cos^2(\theta) + v^2)^{-\frac{\beta}{2}}}{1 + s p_s (r^2 \cos^2(\theta) + v^2)^{-\frac{\beta}{2}}} - \frac{2\mu_r s p_r (r^2 \cos^2(\theta) + v^2)^{-\frac{\beta}{2}}}{1 + s p_r (r^2 \cos^2(\theta) + v^2)^{-\frac{\beta}{2}}} dv} d\theta \quad (18)$$

$$4\lambda_l \mu_r r \int_0^{\pi/2} e^{-2r(\mu_s + \mu_r) \sin(\theta) - \int_r^\infty \sin(\theta) \frac{2\mu_s s p_s (r^2 \cos^2(\theta) + v^2)^{-\frac{\beta}{2}}}{1 + s p_s (r^2 \cos^2(\theta) + v^2)^{-\frac{\beta}{2}}} - \frac{2\mu_r s p_r (r^2 \cos^2(\theta) + v^2)^{-\frac{\beta}{2}}}{1 + s p_r (r^2 \cos^2(\theta) + v^2)^{-\frac{\beta}{2}}} dv} d\theta \quad (19)$$

$$\int_0^\infty J_1(r) e^{-2\lambda_l \int_0^r 1 - J_2(r, v) dv} e^{-2\lambda_l \int_r^\infty 1 - J_3(r, v) dv} dr + \int_0^\infty K_1(r) e^{-2\lambda_l \int_0^r 1 - K_2(r, v) dv - 2\lambda_l \int_r^\infty 1 - K_3(r, v) dv} K_4(r) dr \quad (20)$$

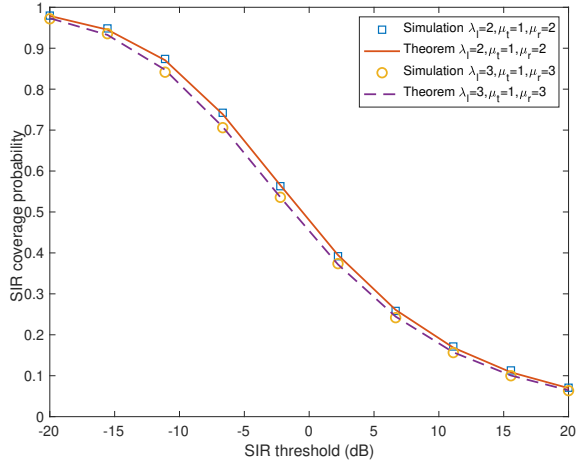


Fig. 6. The derived formula matches the simulation results. We use $\gamma = 1$, $\alpha = 2.5$ and $\beta = 3.5$. The units of λ_l , μ_s , and μ_r are per kilometer.

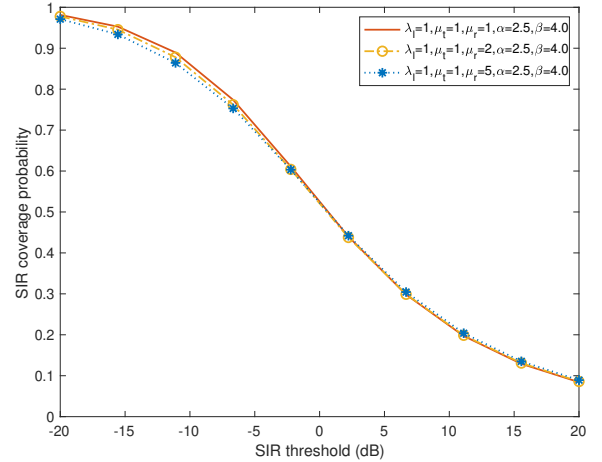


Fig. 7. The illustration of the SIR coverage probability. Here, λ_l and μ_s are fixed whereas μ_r varies.

received signal power and this explains the decrement of the SIR curve as λ_l increases.

In Fig. 9, we increase the road density λ_l and the linear density of relays μ_r at the same rate. In both of pictures, increasing the road density decreases the SIR curve. It is important to mention that the SIR curve decrease in $\alpha = \beta$ is less significant than the SIR curve decrease in $\alpha \neq \beta$. By comparing the top figures of Fig. 7 and 9, we see that the SIR curve decrease much clearer in Fig. 9 because, in general, the average number of transmitters per unit area is $\lambda_l(\mu_s + \mu_v)/\pi$ and thus the top figure of Fig. 9 has much more

transmitters than the top figure of Fig. 7, on average. We can conclude that the interference caused by relays is significant for dense urban areas where roads are densely distributed. Nevertheless, by comparing $\lambda_l = 1, \mu_s = 1, \mu_r = 5$ and $\lambda_l = 5, \mu_s = 1, \mu_r = 5$, we see that the SIR curve decrease from $\mu_r = 1$ to $\mu_r = 5$ is about 15 – 20% when the SIR threshold is between -10 dB and 0 dB. When the SIR threshold is not within this range, the decrease is between 5 – 10%. From these observations, we conclude that despite some SIR decrease, relays are able to redistribute the users that are previously associated with RSUs. In the right picture of Fig. 9,

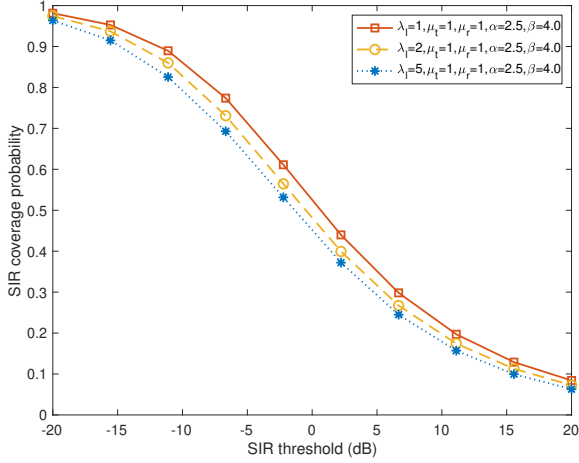


Fig. 8. The illustration of the SIR coverage probability. Here, μ_s and μ_r are fixed whereas λ_l varies.

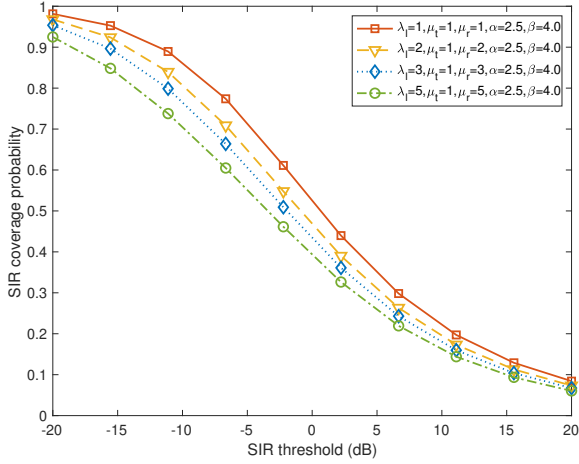


Fig. 9. The SIR coverage probability. We use $\alpha \neq \beta$.

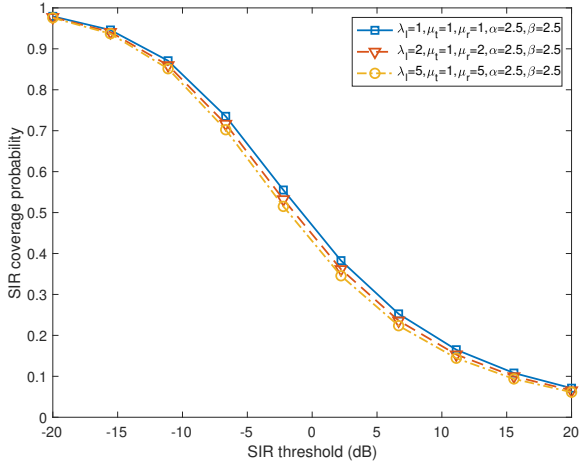


Fig. 10. The SIR coverage probability. We use $\alpha = \beta$.

users are more likely to be associated with relays as the relay density increases. Especially, in the low SIR regime, users are associated with relays on different roads. Consequently, if the cross-road attenuation is not very significant, the received signal power from the association relays increases as we increase the number of relays and it compensates the interference from added relays to some extent. It is worthwhile to stress that such a behavior of the SIR curves exists as long as the density of RSUs or relays is not too high. For instance, a truncated path loss model should be used if transmitters and receivers are too close to each other.

Corollary 1. When $p_s = p_r$, or $\gamma = 1$, the coverage probability of the typical user is given by Eq. (20) where

$$J_1(r) = 2(\mu_s + \mu_r) e^{-2r(\mu_s + \mu_r)} - 2(\mu_s + \mu_r) \int_r^\infty \frac{\tau r^\alpha u^{-\alpha}}{1 + \tau r^\alpha u^{-\alpha}} du,$$

$$J_2(r, v) = e^{-2(\mu_s + \mu_r)\sqrt{r^2 - v^2}} e^{-2(\mu_s + \mu_r) \int_{\sqrt{r^2 - v^2}}^\infty \frac{\tau r^\alpha (v^2 + u^2)^{-\frac{\beta}{2}}}{1 + \tau r^\alpha (v^2 + u^2)^{-\frac{\beta}{2}}} du},$$

$$J_3(r) = e^{-2(\mu_s + \mu_r) \int_0^\infty \frac{\tau r^\alpha (v^2 + u^2)^{-\beta/2}}{1 + \tau r^\alpha (v^2 + u^2)^{-\beta/2}} du},$$

and

$$K_1(r) = e^{-2(\mu_s + \mu_r)r} - 2(\mu_s + \mu_r) \int_r^\infty \frac{\tau r^\beta u^{-\alpha}}{1 + \tau r^\beta u^{-\alpha}} du,$$

$$K_2(r, v) = e^{-2(\mu_s + \mu_r)\sqrt{r^2 - v^2}} e^{-2(\mu_s + \mu_r) \int_{\sqrt{r^2 - v^2}}^\infty \frac{\tau r^\beta (v^2 + u^2)^{-\beta/2}}{1 + \tau r^\beta (v^2 + u^2)^{-\beta/2}} du},$$

$$K_3(r) = e^{-2(\mu_s + \mu_r) \int_0^\infty \frac{\tau r^\beta (v^2 + u^2)^{-\beta/2}}{1 + \tau r^\beta (v^2 + u^2)^{-\beta/2}} du},$$

$$K_4(r) = \int_0^{\pi/2} 4\lambda_l(\mu_s + \mu_r)r e^{-2(\mu_s + \mu_r)r \sin(\theta)} e^{-2(\mu_s + \mu_r) \int_{r \sin(\theta)}^\infty \frac{\tau r^\beta (r^2 \cos^2(\theta) + v^2)^{-\beta/2}}{1 + \tau r^\beta (r^2 \cos^2(\theta) + v^2)^{-\beta/2}} dv} d\theta.$$

Proof: Having $\gamma = 1$ in Theorem 2 completes proof. ■

B. Coverage Probability of the Typical Relay

In practice, relays can serve users only when the relevant data are channeled through RSU-to-relay links. To evaluate the network user performance restricted by the RSU-to-relay links, this section evaluate the coverage probability of the typical relay.

Theorem 3. The coverage probability of the typical relay is given by Eq. (23) where

$$\bar{J}_1(r) = 2\mu_s e^{-2r\mu_s} - 2\mu_s \int_r^\infty \frac{\tau r^\alpha u^{-\alpha}}{1 + \tau r^\alpha u^{-\alpha}} du,$$

$$\bar{J}_2(r, v) = e^{-2\mu_s \sqrt{r^2 - v^2}} - 2\mu_s \int_{\sqrt{r^2 - v^2}}^\infty \frac{\tau r^\alpha (v^2 + u^2)^{-\frac{\beta}{2}}}{1 + \tau r^\alpha (v^2 + u^2)^{-\frac{\beta}{2}}} du},$$

$$\bar{J}_3(r) = e^{-2\mu_s \int_0^\infty \frac{\tau r^\alpha (v^2 + u^2)^{-\beta/2}}{1 + \tau r^\alpha (v^2 + u^2)^{-\beta/2}} du},$$

and

$$\begin{aligned}\bar{K}_1 &= e^{-2r\mu_s - 2\mu_s \int_r^\infty \frac{\tau r^\beta u^{-\alpha}}{1 + \tau r^\beta u^{-\alpha}} du}, \\ \bar{K}_2(r, v) &= e^{-2\mu_s \sqrt{r^2 - v^2} - 2\mu_s \int_{\sqrt{r^2 - v^2}}^\infty \frac{\tau r^\beta (v^2 + u^2)^{-\beta/2}}{1 + \tau r^\beta (v^2 + u^2)^{-\beta/2}} du}, \\ \bar{K}_3(r) &= e^{-2\mu_s \int_0^\infty \frac{\tau r^\beta (v^2 + u^2)^{-\beta/2}}{1 + \tau r^\beta (v^2 + u^2)^{-\beta/2}} dv}, \\ \bar{K}_4(r) &= \int_0^{\pi/2} 4\lambda_l \mu_s r e^{-2\mu_s r \sin(\theta)} \\ &\quad e^{-2\mu_s \int_{r \sin(\theta)}^\infty \frac{\tau r^\beta (r^2 \cos^2(\theta) + v^2)^{-\beta/2}}{1 + \tau r^\beta (r^2 \cos^2(\theta) + v^2)^{-\beta/2}} dv} d\theta.\end{aligned}$$

Proof: We have the result by using techniques in the proof of Theorem 2. ■

We combine Theorem 1, Lemma 1, Theorems 2, and 3 to derive the user throughput.

V. USER THROUGHPUT

In the proposed network, users are associated with either RSUs or relays.

Firstly, the normalized achievable rate of RSU-associated users is defined by the mean achievable rate of the typical RSU-associated users, divided by the mean number of users per RSU. The normalized achievable rate of the RSU-associated user is given by

$$\mathcal{T}_s = \frac{W_1 \mathbf{E}[\log_2(1 + \text{SIR}_{s \rightarrow u})]}{\mathbf{E}[\# \text{ users per RSU}]}. \quad (21)$$

The normalized achievable rate is in a heuristic metric because it is given by the ratio of the achievable rate to the average number of users, not the exact number. However, the exact distribution of the Cox-Voronoi cell is unknown; and thus using the exact number of users per RSU is infeasible. Here, we leverage the mass transport principle to obtain the mean number of users in the typical RSU cell (Theorem 1) and use it to compute the normalized achievable rate of RSU-associated user.

Secondly, the normalized achievable rate of relay-associated users is dictated by both the coverage probabilities of the RSU-to-relay and relay-to-user links. Using the coverage probabilities of the both links, the normalized achievable rate of the relay-associated user is defined by

$$\mathcal{T}_r = \min \left\{ \frac{W_2 \mathbf{E}[\log_2(1 + \text{SIR}_{s \rightarrow r})]}{\mathbf{E}[\# \text{ relay per RSU}] \mathbf{E}[\# \text{ user per relay}]}, \frac{W_1 \mathbf{E}[\log_2(1 + \text{SIR}_{r \rightarrow u})]}{\mathbf{E}[\# \text{ user per relay}]} \right\}, \quad (22)$$

where W_2 is the bandwidth for the RSU-to-relay links and W_1 is the bandwidth for RSU-to-user and relay-to-user links.

Finally, $\mathcal{T} = \mathbf{P}_U^0(A_s) \mathcal{T}_s + \mathbf{P}_U^0(A_r) \mathcal{T}_r$ where $\mathbf{P}_U^0(A_s)$ and $\mathbf{P}_U^0(A_r)$ are given by Theorem 1.

Remark 5. The instantaneous SIRs of RSU-to-relays links do not directly dictate the user throughput. However, these links indirectly affect the user performance by restricting the amount of data available at relays. Consequently, the throughput of relay-associated users will be determined by (i) the throughput of RSU-to-relay links, (ii) the throughput of relay-to-user links,

(iii) the bandwidths W_1 and W_2 , and (iv) the number of relays per RSU and the number of users per relay.

Theorem 4. The user throughput is given by

$$\begin{aligned}\mathcal{T} &= \mathbf{P}_U^0(A_s) W_1 \int_0^\infty \frac{\mathbf{P}_U^0(\text{SIR}_{s \rightarrow u} > 2^\xi - 1)}{\bar{u}_s} d\xi \\ &\quad + \mathbf{P}_U^0(A_r) \min \left\{ \int_0^\infty \frac{W_2 \mathbf{P}_R^0(\text{SIR}_{s \rightarrow r} > 2^\xi - 1)}{\bar{r}_s \bar{u}_r} d\xi, \int_0^\infty \frac{W_1 \mathbf{P}_U^0(\text{SIR}_{r \rightarrow u} > 2^\xi - 1)}{\bar{u}_r} d\xi \right\},\end{aligned}$$

where $\mathbf{P}_U^0(A_s)$ and $\mathbf{P}_R^0(\text{SIR}_{s \rightarrow r} > 2^\xi - 1)$ are given by Theorems 1 and 3, respectively. Using the functions in Theorem 2, the coverage probability of the RSU-associated typical user is given by Eq. (24). Similarly, the coverage probability of the relay-associated typical user is given by Eq. (25). Using Theorem 1, we have $\bar{u}_s = \mu_u \mathbf{P}_U^0(A_s) / \mu_s$, $\bar{u}_r = \mu_u \mathbf{P}_U^0(A_r) / \mu_r$, and $\bar{r}_s = \mu_r / \mu_s$.

Proof: The coverage probabilities of the typical RSU-to-user link and of the typical relay-to-user link are obtained by leveraging Theorem 2, respectively. To obtain \bar{u}_s, \bar{u}_r , and \bar{r}_s , we use Theorem 1. This completes the proof. ■

Example 2. Suppose $\gamma = 1$ and W_2 is sufficiently large. Then, the user throughput is

$$\begin{aligned}\mathcal{T} &= W_1 \int_0^\infty \frac{\mu_s \mathbf{P}_U^0(\text{SIR}_{S \rightarrow U} > 2^\xi - 1)}{\mu_u} d\xi \\ &\quad + W_1 \int_0^\infty \frac{\mu_r \mathbf{P}_U^0(\text{SIR}_{R \rightarrow U} > 2^\xi - 1)}{\mu_u} d\xi. \quad (26)\end{aligned}$$

On the other hand, the user throughput without any relay is

$$\left(\frac{\mu_s}{\mu_u} \right) W_1 \int_0^\infty \mathbf{P}_U^0(\text{SIR} > 2^\xi - 1) d\xi. \quad (27)$$

As a result, based on Eqs. (26) and (27), the proposed network has a multiplicative gain Γ in the user throughput given by

$$\begin{aligned}\Gamma &= \frac{\int_0^\infty \mathbf{P}_U^0(\text{SIR}_{S \rightarrow U} > 2^\xi - 1) d\xi}{\int_0^\infty \mathbf{P}_U^0(\text{SIR} > 2^\xi - 1) d\xi} \\ &\quad + \left(\frac{\mu_r}{\mu_s} \right) \frac{\int_0^\infty \mathbf{P}_U^0(\text{SIR}_{R \rightarrow U} > 2^\xi - 1) d\xi}{\int_0^\infty \mathbf{P}_U^0(\text{SIR} > 2^\xi - 1) d\xi}.\end{aligned}$$

Remark 6. Theorem 4 shows the user throughput as a function of W_1, W_2 , and the distributions of $\text{SIR}_{S \rightarrow U}, \text{SIR}_{R \rightarrow U}$, and $\text{SIR}_{S \rightarrow R}$. It shows when W_2 is large, deploying relays will increase the user throughput of the network or the normalized achievable rate of user. In many cases where $W_1 + W_2 = W$, the derived user throughput formula is useful to the understanding tradeoff relationship between network parameters and addressing design problems exist in heterogeneous vehicular networks. For instance, to maximize the user throughput, one can find the optimal density of relays for a given W_2 . Similarly, when the density of relays is given, one can use the user throughput formula to study the impact of W_2 .

Fig. 11 shows the user throughput in Theorem 4 where we use $W = 20$ MHz, $\lambda_l = 3/\text{km}$, $\mu_s = 1/\text{km}$, $\mu_r = 3/\text{km}$, $\mu_u = 15/\text{km}$, $\alpha = 2.5$, and $\beta = 3.5$. It shows that for

$$\int_0^\infty \bar{J}_1(r) e^{-2\lambda_l \int_0^r 1 - \bar{J}_2(r,v) dv} e^{-2\lambda_l \int_r^\infty 1 - \bar{J}_3(r,v) dv} dr + \int_0^\infty \bar{K}_1(r) e^{-2\lambda_l \int_0^r 1 - \bar{K}_2(r,v) dv} e^{-2\lambda_l \int_r^\infty 1 - \bar{K}_3(r,v) dv} \bar{K}_4(r) dr. \quad (23)$$

$$\frac{1}{\mathbf{P}_U^0(\mathcal{A}_s)} \int_0^\infty G_1(r, a, b) e^{-2\lambda_l \int_0^r 1 - G_2(r,v,a,b) dv} e^{-2\lambda_l \int_r^\infty 1 - G_3(r,v,a,b) dv} dr \Big|_{a=1, b=\frac{1}{\gamma}} + \frac{1}{\mathbf{P}_U^0(\mathcal{A}_s)} \int_0^\infty H_1(r, a, b) e^{-2\lambda_l \int_0^r 1 - H_2(r,v,a,b) dv} e^{-2\lambda_l \int_r^\infty 1 - H_3(r,v,a,b) dv} H_4(r, a, b) dr \Big|_{a=1, b=\frac{1}{\gamma}, c=\mu_s}. \quad (24)$$

$$\frac{1}{\mathbf{P}_U^0(\mathcal{A}_r)} \int_0^\infty G_1(r, a, b) e^{-2\lambda_l \int_0^r 1 - G_2(r,v,a,b) dv} e^{-2\lambda_l \int_r^\infty 1 - G_3(r,v,a,b) dv} dr \Big|_{a=\gamma, b=1} + \frac{1}{\mathbf{P}_U^0(\mathcal{A}_r)} \int_0^\infty H_1(r, a, b) e^{-2\lambda_l \int_0^r 1 - H_2(r,v,a,b) dv} e^{-2\lambda_l \int_r^\infty 1 - H_3(r,v,a,b) dv} \bar{H}_4(r, a, b) dr \Big|_{a=\gamma, b=1, c=\mu_r}. \quad (25)$$

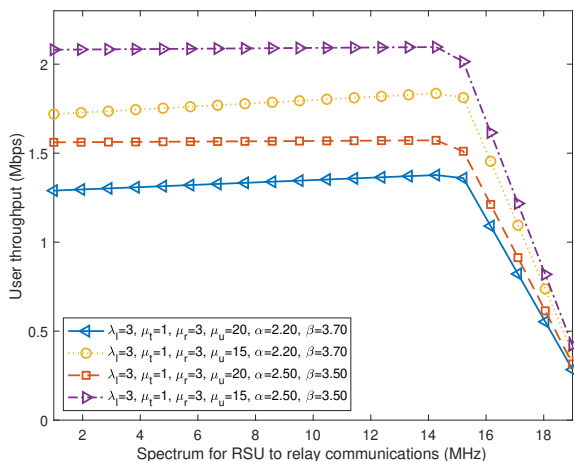


Fig. 11. User throughput in Theorem 4.

the given network parameters, $W_2 = 14$ maximizes the user throughput of the proposed two-tier heterogeneous vehicular network. Note the maximum value of W_2 varies depending on the network variables such as λ_l , μ_s , μ_r , α and β . In practice, by exploiting Theorem 4 network operators can easily find the optimal solution for W_2 with a marginally little computation cost.

VI. CONCLUSION AND FUTURE WORK

Using stochastic geometry, this paper proposes and analyzes a novel two-tier heterogeneous vehicular network architecture where RSUs and vehicular relays serve network users. By assuming such vehicular relays are operated by RSUs and users are associated with either RSUs or relays, we derive the association probability of the network users. We find that the association probability is a nonlinear function of the RSU and relay densities because RSUs, relays, and users are all on roads. Then, we derive the coverage probability of the typical user and then obtain the user throughput. In particular, the user throughput incorporates the fact that RSUs operate relays and that the throughput of relay-associated users is

dictated by the SIRs of RSU-to-relay and relay-to-user links and the corresponding bandwidths for those links. The paper gives practical insights on designing heterogeneous vehicular networks with RSUs and vehicular relays. By presenting the formulas for SIR and user throughput as network parameters, one can easily identify the complex interactions occur at the network and use these formulas to enhance reliability or to increase throughput.

The present paper starts a new line of studies on heterogeneous vehicular networks. It provides a tractable model and a tool to analyzing the network performance. The analysis of this paper can be developed further by considering new and more practical components; for instance, the clustering of vehicles on roads can be represented by an independent cluster point process on roads. The analysis of the proposed two-tier heterogeneous vehicular network is applicable to the analysis of multi-tier vehicular networks where there are various types of network elements exist such as RSUs, relays, and IoT devices.

APPENDIX PROOF OF THEOREM 2

Proof: Under the Palm distribution of the user point process, $\mathbf{P}_U^0(\cdot)$, there exist a typical user at the origin and a line $l(0, \theta_0)$ containing the typical user. Here, θ_0 is a uniform random variable between 0 and π . By the law of total probability, the coverage probability is given by

$$\mathbf{P}_U^0(\text{SIR} > \tau) = \mathbf{P}_U^0(\text{SIR} > \tau, E) + \mathbf{P}_U^0(\text{SIR} > \tau, E^c), \quad (28)$$

where we can write $E : \{l_\star = l(0, \theta_0)\}$ and $E^c : \{l_\star \neq l(0, \theta_0)\}$. The former is the event that the line l_\star containing the association transmitter is $l(0, \theta_0)$, the line that contains the typical user.

$$\mathbf{P}_U^0(\text{SIR} > \tau, E) = \mathbf{P}_U^0(\text{SIR} > \tau, E, A_s) + \mathbf{P}_U^0(\text{SIR} > \tau, E, A_r), \quad (29)$$

where A_s and A_r are the events that the typical user is associated with its closest RSU and with its closest relay,

respectively. Then, with I the interference seen by the typical user, we have

$$\begin{aligned}
& \mathbf{P}(\text{SIR} > \tau, E, A_s) \\
&= \mathbf{P}_U^0(p_s H L(\|X^*\|) > \tau I, E, A_s) \\
&= \mathbf{P}_U^0(p_s H > \tau I \|X^*\|^\alpha, E, A_s) \\
&= \mathbf{E}_\Phi \left[\mathbf{P}_U^0 \left(H > \frac{\tau I \|X^*\|^\alpha}{p_s}, E, A_s \mid \Phi \right) \right] \\
&= \mathbf{E}_\Phi \left[\int_{r=0}^{r=\infty} \mathbf{P}_U^0 \left(H > \frac{\tau r^\alpha I}{p_s} \mid E, A_s, \|X_S^*\| = r, \Phi \right) \right. \\
&\quad \left. \mathbf{P}(\|X_S^*\| \in [r, r + dr), E, A_s \mid \Phi) \right], \quad (30)
\end{aligned}$$

where we express the probability as the conditional expectation w.r.t. Φ . Then, we write it as a conditional expectation w.r.t. the nearest RSU. We have $\mathbf{P}(\|X_S^*\| = r dr, E, A_s \mid \Phi)$ the conditional probability density function of the distance from the origin to the closest RSU.

In a similar way, we have

$$\begin{aligned}
& \mathbf{P}(\text{SIR} > \tau, E, A_r) \\
&= \mathbf{E}_\Phi \left[\int_{r=0}^{r=\infty} \mathbf{P}_U^0 \left(H > \frac{\tau r^\alpha I}{p_r} \mid E, A_r, \|X_R^*\| = r, \Phi \right) \right. \\
&\quad \left. \mathbf{P}(\|X_R^*\| \in [r, r + dr), E, A_r \mid \Phi) \right]. \quad (31)
\end{aligned}$$

In Eq. (31), $\mathbf{P}(\|X_R^*\| \in [r, r + dr), E, A_r \mid \Phi)$ is the conditional probability density function of the distance from the origin to the nearest relay. Furthermore, the integrands of Eqs. (30) and (31) are

$$\begin{aligned}
& \mathbf{P}_U^0 \left(H > \frac{\tau r^\alpha I}{p_s} \mid E, A_s, r, \Phi \right) \\
&= \mathbf{E}_U^0 [e^{-sI} \mid E, A_s, r, \Phi] \Big|_{s=\tau r^\alpha p_s^{-1}}, \quad (32)
\end{aligned}$$

$$\begin{aligned}
& \mathbf{P}_U^0 \left(H > \frac{\tau r^\alpha I}{p_r} \mid E, A_r, r, \Phi \right) \\
&= \mathbf{E}_U^0 [e^{-sI} \mid E, A_r, r, \Phi] \Big|_{s=\tau r^\alpha p_r^{-1}}, \quad (33)
\end{aligned}$$

respectively. We obtain

$$\mathbf{E}_U^0 [e^{-sI} \mid E, A_s, r, \Phi] = \mathbf{E}_U^0 [e^{-sI} \mid E, A_r, r, \Phi]$$

from the independence of the Poisson point processes. The conditional Laplace transform of interference is given by

$$\mathbf{E}_U^0 [e^{-sI} \mid E, A_s, r, \Phi] \quad (34)$$

$$\begin{aligned}
&= \prod_{T_k \in S_{0,\theta_0} + R_{0,\theta_0}}^{|T_k| > r} \left(\frac{1}{1 + sp \|T_k\|^{-\frac{\beta}{2}}} \right) \\
&\quad \prod_{r_i, \theta_i \in \Phi \setminus \{0, \theta_0\}} \left(\prod_{T_k \in S_{r_i, \theta_i} + R_{r_i, \theta_i}}^{|T_k| > r} \frac{1}{1 + sp \|T_k\|^{-\frac{\beta}{2}}} \right)
\end{aligned}$$

where we use the Laplace transform of the exponential random variable and the fact that conditionally on the line process and

conditionally on the association distance r , all RSUs and relays are at distances greater than r . Then, we have

$$\begin{aligned}
& \mathbf{E}_U^0 [e^{-sI} \mid E, A_s, r, \Phi] \\
&= e^{-2\mu_s \int_r^\infty \frac{sp_s u^{-\alpha}}{1 + sp_s u^{-\alpha}} du - 2\mu_r \int_r^\infty \frac{sp_r u^{-\alpha}}{1 + sp_r u^{-\alpha}} du} \\
&\quad \times \prod_{\substack{|r_i| < r \\ r_i \in \Phi}} \left(e^{-2\mu_s \int_{\sqrt{r^2 - r_i^2}}^\infty \frac{sp_s (r_i^2 + u^2)^{-\frac{\beta}{2}}}{1 + sp_s (r_i^2 + u^2)^{-\frac{\beta}{2}}} du} \right. \\
&\quad \left. e^{-2\mu_r \int_{\sqrt{r^2 - r_i^2}}^\infty \frac{sp_r (r_i^2 + u^2)^{-\frac{\beta}{2}}}{1 + sp_r (r_i^2 + u^2)^{-\frac{\beta}{2}}} du} \right) \\
&\quad \times \prod_{\substack{|r_i| > r \\ r_i \in \Phi}} \left(e^{-2\mu_s \int_0^\infty \frac{sp_s (r_i^2 + u^2)^{-\frac{\beta}{2}}}{1 + sp_s (r_i^2 + u^2)^{-\frac{\beta}{2}}} du} \right. \\
&\quad \left. e^{-2\mu_r \int_0^\infty \frac{sp_r (r_i^2 + u^2)^{-\frac{\beta}{2}}}{1 + sp_r (r_i^2 + u^2)^{-\frac{\beta}{2}}} du} \right). \quad (35)
\end{aligned}$$

where we use the facts that RSU and relay point processes on different lines are conditionally independent and that the distances from the origin to any RSU points $\{T_k\}_{k \in \mathbb{Z}} \in S_{r_i, \theta_i}$ are given by $\{\sqrt{r_i^2 + G_k^2}\}_{k \in \mathbb{Z}}$, where $\{G_k\}_{k \in \mathbb{Z}}$ is the RSU Poisson point process on the real axis $S_{0,0}$.

On the other hand, the probability density function in Eq. (30) is given by

$$\begin{aligned}
& \mathbf{P}(\|X_S^*\| \in [r, r + dr), E, A_s \mid \Phi) \\
&= \frac{\partial(1 - \mathbf{P}(S_{0,\theta_0}(B_0(r)) = 0))}{\partial r} \\
&\quad \times \mathbf{P}(R_{0,\theta_0}(B(r)) = \emptyset) \prod_{r_i, \theta_i \in \Phi} \mathbf{P}(S_{r_i, \theta_i} + R_{r_i, \theta_i}(B(r)) = \emptyset) \\
&= 2\mu_s e^{-2r\mu_s} dr e^{-2r\mu_r} \prod_{\substack{|r_i| < r \\ r_i, \theta_i \in \Phi}} e^{-2(\mu_s + \mu_r) \sqrt{r^2 - r_i^2}},
\end{aligned}$$

where we use the facts that (i) $X^* \in S_{0,\theta_0}$ and (ii) there is no point of $R_{0,\theta_0} + S_{r_i, \theta_i} + R_{r_i, \theta_i}$ within a disk of radius r centered at the origin. The probability density function in Eq. (31) is

$$\begin{aligned}
& \mathbf{P}(\|X_R^*\| \in (r, r + dr), E, A_r \mid \Phi) \\
&= 2\mu_r e^{-2r\mu_r} dr e^{-2r\mu_s} \prod_{\substack{|r_i| < r \\ r_i, \theta_i \in \Phi}} e^{-2(\mu_s + \mu_r) \sqrt{r^2 - r_i^2}}. \quad (36)
\end{aligned}$$

To obtain the first part of Eq. (28), we combine Eqs. (31) – (36).

Let us now evaluate the second part of Eq. (28). By the law of total probability, the expression $\mathbf{P}_U^0(\text{SIR} > \tau, E^c)$ is

$$\mathbf{P}_U^0(\text{SIR} > \tau, E^c, A_s) + \mathbf{P}_U^0(\text{SIR} > \tau, E^c, A_r) \quad (37)$$

where A_s and A_r denote the events that the typical user is associated with the RSU or with the relay, respectively. Let l_* denote the line of the association RSU transmitter. Then, by

conditioning on Φ , on l_* , and then $\|X_S^*\|$, we can write the first part of Eq. (37) as follows:

$$\begin{aligned} & \mathbf{P}_U^0(\text{SIR} > \tau, E^c, A_s) \\ &= \mathbf{P}_U^0(p_s H > \tau I \|X_*\|^\beta, E^c, A_s) \\ &= \mathbf{E}_\Phi \left[\mathbf{P}_U^0 \left(H > \frac{\tau I \|X_*\|^\beta}{p_s}, E^c, A_s \mid \Phi \right) \right] \\ &= \mathbf{E}_{\Phi, l_*} \left[\mathbf{P}_U^0 \left(H > \frac{\tau I \|X_S^*\|^\beta}{p_s}, E^c, A_s \mid l_*, \Phi \right) \right] \\ &= \mathbf{E}_{\Phi, l_*, r} \left[\mathbf{P}_U^0 \left(H > \frac{\tau r^\beta I}{p_s} \mid E^c, A_s, r, l_* \Phi \right) \right], \quad (38) \end{aligned}$$

where we write $\|X_S^*\| = r$.

In a similar way, the second part of Eq. (37) is given by

$$\begin{aligned} & \mathbf{P}_U^0(\text{SIR} > \tau, E^c, A_r) \\ &= \mathbf{E}_{\Phi, l_*, r} \left[\mathbf{P}_U^0 \left(H > \frac{\tau r^\beta I}{p_r} \mid E^c, A_r, r, l_* \Phi \right) \right], \quad (39) \end{aligned}$$

where we write $\|X_R^*\| = r$.

By using the fact that H is an exponential random variable, the conditional probability of Eq. (38) is given by expression (17) where the distances from the origin to the points of the Poisson point process on line $l(r_i, \theta_i)$ are represented by $\|r_i \bar{e}_1 + T_j \bar{e}_2\|$ where $\bar{e}_{i,1}$ is a unit 1 orthogonal vector from the origin to the line $l(r_i, \theta_i)$ and $\bar{e}_{i,2}$ is a unit 1 vector, orthogonal to the vector $\bar{e}_{i,1}$. Here, $S_{0,0}$ is the RSU point process on the x -axis and $R_{0,0}$ is the relay point process on the x -axis. By using the probability generating functional of the Poisson point process, we have

$$\begin{aligned} \mathcal{L}_I(s) &= e^{\left(-2\mu_s \int_r^\infty \frac{p_s s v^{-\alpha}}{1+p_s s v^{-\alpha}} dv - 2\mu_r \int_r^\infty \frac{p_r s v^{-\alpha}}{1+p_r s v^{-\alpha}} dv\right)} \\ &\times \prod_{\substack{|r_i| < r \\ r_i, \theta_i \in \Phi + \delta_{r_*, \theta_*}}} e^{\left(-2\mu_s \int_{\sqrt{r^2 - r_i^2}}^\infty \frac{p_s s (r_i^2 + v^2)^{-\frac{\beta}{2}}}{1+p_s s (r_i^2 + v^2)^{-\frac{\beta}{2}}} dv\right)} \\ &\times \prod_{\substack{|r_i| < r \\ r_i, \theta_i \in \Phi + \delta_{r_*, \theta_*}}} e^{\left(-2\mu_r \int_{\sqrt{r^2 - r_i^2}}^\infty \frac{p_r s (r_i^2 + v^2)^{-\frac{\beta}{2}}}{1+p_r s (r_i^2 + v^2)^{-\frac{\beta}{2}}} dv\right)} \\ &\times \prod_{\substack{|r_i| > r \\ r_i, \theta_i \in \Phi}} e^{\left(-2\mu_s \int_0^\infty \frac{p_s s (r_i^2 + v^2)^{-\frac{\beta}{2}}}{1+p_s s (r_i^2 + v^2)^{-\frac{\beta}{2}}} dv\right)} \\ &\times \prod_{\substack{|r_i| > r \\ r_i, \theta_i \in \Phi}} e^{\left(-2\mu_r \int_0^\infty \frac{p_r s (r_i^2 + v^2)^{-\frac{\beta}{2}}}{1+p_r s (r_i^2 + v^2)^{-\frac{\beta}{2}}} dv\right)}, \quad (40) \end{aligned}$$

where the above five terms of Eq. (40) correspond to the Laplace transforms of the interference of (i) RSU plus relay on the line $l(0, \theta_0)$, (ii) RSU on the lines closer than r , (iii) relay on the lines closer than r , (iv) RSU on the lines further than r , and (v) relay on the lines further than r , respectively.

To obtain the conditional probability density function of the distance from the origin to its closest RSU in Eq. (38), we use the facts that (i) X_S^* is the closest to the origin, (ii) $X_S^* \in S_{r_*, \theta_*}$, and (iii) all the other RSU or relay point processes have no point in the disk of radius r . Therefore, using the void probability of the Poisson point process, the conditional

probability density function of the distance from the origin to its closest RSU in Eq. (38) is

$$\begin{aligned} & \mathbf{P}_U^0(\|X_S^*\| \in [r, r + dr), E^c, A_s | l^*, \Phi) \\ &= \frac{d}{dr} (1 - \mathbf{P}(S_{r_*, \theta_*}(B(r)) = \emptyset)) dr \mathbf{P}(R_{r_*, \theta_*}(B(r)) = \emptyset) \\ &\quad \times \left(\prod_{r, \theta}^{\Phi + l_0} \mathbf{P}(R_{r, \theta} + S_{r, \theta}(B(r)) = \emptyset) \right) \\ &= \frac{2\mu_s r e^{-2(\mu_s + \mu_r) \sqrt{r^2 - r_*^2}}}{\sqrt{r^2 - r_*^2}} dr \prod_{r_i, \theta_i}^{\Phi + \delta_0, \theta_0} e^{-2(\mu_s + \mu_r) \sqrt{r^2 - r_i^2}}. \quad (41) \end{aligned}$$

In a similar way, the conditional probability density function of the distance from the origin to its closest relay in Eq. (39) is given by

$$\begin{aligned} & \mathbf{P}_U^0(\|X_S^*\| \in [r, r + dr), E^c, A_r | l^*, \Phi) \\ &= \frac{2\mu_r r e^{-2(\mu_s + \mu_r) \sqrt{r^2 - r_*^2}}}{\sqrt{r^2 - r_*^2}} dr \prod_{r_i}^{\Phi + \delta_0, \theta_0} e^{-2(\mu_s + \mu_r) \sqrt{r^2 - r_i^2}}. \quad (42) \end{aligned}$$

Finally, we combine Eqs. (40) and (41) then integrate the result w.r.t. l_* and then w.r.t. Φ . First, to integrate w.r.t. l_* , we combine all the functions w.r.t. l_* to get the expression (18). Then, we combine Eqs. (40), (41), and (18).

Similarly, to obtain the second part of Eq. (37), we combine Eq. (40) and (42) and evaluate the functions w.r.t. l_* to obtain Eq. (19). Then, we combine the rest of Eq. (40), (42) and (19) to complete the proof. ■

ACKNOWLEDGMENT

The work of Chang-Sik Choi was supported in part by the NRF-2021R1F1A1059666. The work of Francois Baccelli was supported by the ERC NEMO grant 788851 to INRIA.

REFERENCES

- [1] C.-S. Choi, "User association in a heterogeneous vehicular network with roadside units and vehicle relays," *IEEE Wireless Commun. Lett.*, vol. 11, no. 11, pp. 2345–2349, 2022.
- [2] J. B. Kenney, "Dedicated short-range communications (DSRC) standards in the United States," *Proceedings of the IEEE*, vol. 99, no. 7, pp. 1162–1182, July 2011.
- [3] J. Jin, J. Gubbi, S. Marusic, and M. Palaniswami, "An information framework for creating a smart city through Internet of Things," *IEEE Internet Things J.*, vol. 1, no. 2, pp. 112–121, 2014.
- [4] N. Lu, N. Cheng, N. Zhang, X. Shen, and J. W. Mark, "Connected vehicles: Solutions and challenges," *IEEE Internet Things J.*, vol. 1, no. 4, pp. 289–299, 2014.
- [5] 3GPP TR 36.885, "Study on LTE-based V2X services," *3GPP TR 36.885*.
- [6] S. Chen, J. Hu, Y. Shi, Y. Peng, J. Fang, R. Zhao, and L. Zhao, "Vehicle-to-everything (V2X) services supported by LTE-based systems and 5G," *IEEE Commun. Standards Mag.*, vol. 1, no. 2, pp. 70–76, 2017.
- [7] 3GPP TS 22.816, "Service requirements for enhanced V2X scenarios," *3GPP TS 22.816*.
- [8] 3GPP TR 22.836, "Study on enhancement of 3GPP support for 5G V2X services," *3GPP TR 22.836*.
- [9] M. H. C. Garcia, A. Molina-Galan, M. Boban, J. Gozalvez, B. Coll-Perales, T. Şahin, and A. Kousaridas, "A tutorial on 5G NR V2X communications," *IEEE Commun. Surv&Tuts*, vol. 23, no. 3, pp. 1972–2026, 2021.
- [10] 3GPP TR 38.836, "Study on NR sidelink relay," *3GPP TR 38.836*.

- [11] 3GPP TR 38.874, “NR; study on integrated access and backhaul,” *3GPP TR 38.874*.
- [12] F. Baccelli and S. Zuyev, “Stochastic geometry models of mobile communication networks,” *Frontiers in queueing*, pp. 227–243, 1997.
- [13] D. J. Daley and D. Vere-Jones, *An introduction to the theory of point processes: volume II: general theory and structure*. Springer Science & Business Media, New York, 2007.
- [14] S. N. Chiu, D. Stoyan, W. S. Kendall, and J. Mecke, *Stochastic geometry and its applications*. John Wiley & Sons, 2013.
- [15] M. Haenggi, J. G. Andrews, F. Baccelli, O. Dousse, and M. Franceschetti, “Stochastic geometry and random graphs for the analysis and design of wireless networks,” *IEEE J. Sel. Areas Commun.*, vol. 27, no. 7, pp. 1029–1046, 2009.
- [16] F. Baccelli, B. Błaszczyszyn, and P. Muhlethaler, “An Aloha protocol for multihop mobile wireless networks,” *IEEE Trans. Inf. Theory*, vol. 52, no. 2, pp. 421–436, Feb 2006.
- [17] J. G. Andrews, F. Baccelli, and R. K. Ganti, “A tractable approach to coverage and rate in cellular networks,” *IEEE Trans. Commun.*, vol. 59, no. 11, pp. 3122–3134, 2011.
- [18] H. S. Dhillon, R. K. Ganti, F. Baccelli, and J. G. Andrews, “Modeling and analysis of K-tier downlink heterogeneous cellular networks,” *IEEE J. Sel. Areas Commun.*, vol. 30, no. 3, pp. 550–560, 2012.
- [19] S. Singh, H. S. Dhillon, and J. G. Andrews, “Offloading in heterogeneous networks: Modeling, analysis, and design insights,” *IEEE Trans. Wireless Commun.*, vol. 12, no. 5, pp. 2484–2497, 2013.
- [20] F. Morlot, “A population model based on a Poisson line tessellation,” in *Proc. IEEE WiOpt*, 2012, pp. 337–342.
- [21] V. V. Chetlur and H. S. Dhillon, “Coverage analysis of a vehicular network modeled as Cox process driven by Poisson line process,” *IEEE Trans. Wireless Commun.*, vol. 17, no. 7, pp. 4401–4416, July 2018.
- [22] C.-S. Choi and F. Baccelli, “An analytical framework for coverage in cellular networks leveraging vehicles,” *IEEE Trans. Commun.*, vol. 66, no. 10, pp. 4950–4964, Oct 2018.
- [23] —, “Poisson Cox point processes for vehicular networks,” *IEEE Trans. Veh. Technol.*, vol. 67, no. 10, pp. 10 160–10 165, Oct 2018.
- [24] V. V. Chetlur and H. S. Dhillon, “Success probability and area spectral efficiency of a VANET modeled as a Cox process,” *IEEE Wireless Commun. Lett.*, vol. 7, no. 5, pp. 856–859, 2018.
- [25] C.-S. Choi and F. Baccelli, “Spatial and temporal analysis of direct communications from static devices to mobile vehicles,” *IEEE Trans. Wireless Commun.*, vol. 18, no. 11, pp. 5128–5140, 2019.
- [26] C.-S. Choi, F. Baccelli, and G. de Veciana, “Densification leveraging mobility: An IoT architecture based on mesh networking and vehicles,” in *Proc. IEEE/ACM MobiHoc*, 2018, p. 71–80.
- [27] Y. Sun, Z. Ding, X. Dai, K. Navaie, and D. K. C. So, “Performance of downlink NOMA in vehicular communication networks: An analysis based on Poisson line Cox point process,” *IEEE Trans. Veh. Technol.*, vol. 69, no. 11, pp. 14 001–14 006, 2020.
- [28] C.-S. Choi and F. Baccelli, “Modeling and analysis of vehicle safety message broadcast in cellular networks,” *IEEE Trans. Wireless Commun.*, vol. 20, no. 7, pp. 4087–4099, 2021.
- [29] Y. Sun, Z. Ding, and X. Dai, “On the outage performance of network noma (N-NOMA) modeled by Poisson line Cox point process,” *IEEE Trans. Veh. Technol.*, vol. 70, no. 8, pp. 7936–7950, 2021.
- [30] K. Koufos, H. S. Dhillon, M. Dianati, and C. P. Dettmann, “On the k nearest-neighbor path distance from the typical intersection in the manhattan poisson line cox process,” *IEEE Trans. Mobile Comput.*, vol. 22, no. 3, pp. 1659–1671, 2023.
- [31] S. Kassir, G. de Veciana, N. Wang, X. Wang, and P. Palacharla, “Analysis of opportunistic relaying and load balancing gains through V2V clustering,” *IEEE Trans. Veh. Technol.*, vol. 71, no. 9, pp. 9896–9911, 2022.
- [32] T.-X. Zheng, Y. Wen, H.-W. Liu, Y. Ju, H.-M. Wang, K.-K. Wong, and J. Yuan, “Physical-layer security of uplink mmwave transmissions in cellular V2X networks,” *IEEE Trans. Wireless Commun.*, vol. 21, no. 11, pp. 9818–9833, 2022.
- [33] C.-S. Choi and F. Baccelli, “LOS coverage area in vehicular networks with Cox-distributed roadside units and relays,” *IEEE Trans. Veh. Technol.*, vol. 72, no. 6, pp. 7772–7782, 2023.
- [34] Y. Qin, M. A. Kishk, and M.-S. Alouini, “A dominant interferer plus mean field-based approximation for SINR meta distribution in wireless networks,” *IEEE Trans. Commun.*, vol. 71, no. 6, pp. 3663–3678, 2023.
- [35] 3GPP TR 37.885, “Study on evaluation methodology of new vehicle-to-everything (V2X) use cases for LTE and NR.”
- [36] 3GPP TR 38.211, “NR; physical channels and modulation,” *3GPP TR 38.211*.
- [37] 3GPP TR 38.213, “NR; physical layer procedures for control,” *3GPP TR 38.213*.
- [38] F. Baccelli and B. Błaszczyszyn, “Stochastic geometry and wireless networks: volume I theory,” *Foundations and Trends in Networking*, vol. 3, no. 3–4, pp. 249–449, 2010.
- [39] H.-S. Jo, Y. J. Sang, P. Xia, and J. G. Andrews, “Heterogeneous cellular networks with flexible cell association: A comprehensive downlink sinr analysis,” *IEEE Trans. Wireless Commun.*, vol. 11, no. 10, pp. 3484–3495, 2012.
- [40] S. Singh, F. Baccelli, and J. G. Andrews, “On association cells in random heterogeneous networks,” *IEEE Wireless Commun. Lett.*, vol. 3, no. 1, pp. 70–73, 2014.
- [41] A. Goldsmith, *Wireless communications*. Cambridge University Press, 2005.
- [42] 3GPP TR 38.901, “NR; study on channel model for frequencies from 0.5 to 100 GHz,” *3GPP TR 38.901*.
- [43] F. Baccelli and B. Błaszczyszyn, “Stochastic geometry and wireless networks: Volume II applications,” *Foundations and Trends in Networking*, vol. 4, no. 1–2, pp. 1–312, 2010.
- [44] F. Baccelli and P. Brémaud, *Elements of queueing theory: Palm Martingale calculus and stochastic recurrences*. Springer & Verlag, 2013, vol. 26.